An O-band Polarization-Insensitive SOA Building Block for SOA-Based Optical Switches in IMOS Platform

D.W. Feyisa, Y.Jiao, Z.Chen, N.Calabretta and R.Stabile

Institute for Photonic Integration, Eindhoven University of Technology, P.O. Box 513, 5600MB Eindhoven, the Netherlands.

Abstract

Low loss, compact passive optical components, and high-performance TE optimized multi-quantum well (MQW) semiconductor optical amplifiers (SOAs) have already been demonstrated in the IMOS platform. All of these features but the polarization sensitivity of the SOA make the platform desirable for SOA-based optical switches. This work tries to solve the polarization sensitivity of the SOA and show a polarization-insensitive SOA design in the 1300 nm optical transmission window. The achieved polarization sensitivity is <0.5 dB in 60 nm bandwidth. One of the critical parameters for SOA-based switches, the output saturation power, has been investigated for SOA widths of 1.5 µm and 2.5 µm. A 500 µm long, 2.5 µm wide SOA could provide around 11 dBm output saturation power at 5 kA/cm^2, 2 dB more than a 1.5 µm SOA. The SOA is monolithically co-integrated with passive waveguide using the twin-guide principle with high TE and TM polarization coupling efficiency. Using the designed SOA as a switching element, we emulated a 16×16 SOA-based optical switch using two modular switch architectures: a blocking Banyan and rearrangeable non-blocking Hybrid-Benes architectures. Bit transmission with WDM signals shows that the SOA cascade has good performance in power penalty and on-chip path gain.

1. Introduction

Switching in the optical domain is a pivotal technology to keep pace with the cost, size, latency, and capacity requirements of rapidly growing data center traffic [1]. Semiconductor optical amplifier (SOA)-based switches are potential candidates for such applications as they could leverage the high bandwidth and fast switching capability of SOAs. Even though research on SOA-based switches has shown significant progress over the years, polarization dependency, path loss, and SOA-induced sensitivity power penalty due to noise has been challenging [2]–[4]. Hybrid MZI-SOA based switches have shown promising results in improving loss, extinction ratio, and receiver sensitivity power penalty [4]. However, the use of MZI increases the number of electrodes which may complicate electrical fanout design. Compared to bulk InP/InGaAsP, low loss and compact components have been achieved in the indium phosphide membrane on silicon (IMOS) platform thanks to its high index contrast [5]–[9]. Compactness could increase yield in large radix switches where large-scale photonic integration is needed. Similarly, the reduced component loss could relax the gain requirements and allow short SOAs to improve ASE and input power dynamic range (IPDR), which may help yearn good sensitivity and SOA cascadability.

This paper proposes exploiting the IMOS platform for optical switching applications and explores an O-band PI-SOA design suitable for optical switching applications on the IMOS platform. We use a strained, thin, bulk-active layer to achieve polarization insensitivity. We investigate polarization sensitivity, output saturation power, and 3 dB

gain bandwidth. Finally, We emulate two modular switch architectures using this novel SOA design and study the effect of SOA cascades analyzing the bit error rate for incoming WDM signals at 25 Gb/s.

2. IMOS O-band PI-SOA Design

Generally, polarization-insensitive SOA can be designed using MQW or bulk structures. Quantum well SOAs are generally more efficient but achieving polarization insensitivity is relatively challenging compared to bulk. There are two approaches for polarization insensitivity for bulk structures. The first one uses a square shape: bulk actives have the same material gain for TE and TM, and confinement factors can be manipulated by playing with geometry. The second approach uses a strained active, in which we put a tensile strain in the active region, manipulating material gain.

We use a strained bulk active layer for this work. Fig.1a shows the cross-section of an SOA design. We use InGaAsP (Q1.05) for the separate confinement heterostructure (SCH) to provide sufficient barrier height for providing enough carrier confinement. A thin tensile strained bulk active layer is used to provide polarization independence. In addition to the strain, the choice of the SCH dimensions facilitates polarization insensitivity with less strain by influencing the confinement factor. The overall thickness of the active region (core and SCHs) is 300 nm. The choice of dimensions combined with added 0.18% tensile strain in the active layer provides a similar gain for TE and TM. Fig. 1b depicts the material gain for TE and TM. It can be seen that the TM material gain is enhanced, which is the result of the strain. The active device is monolithically co-integrated with passive waveguides using the twin-guide approach [7]. The active-passive coupling efficiency achieved for the design is 96.5% for TM and 98% for TE.

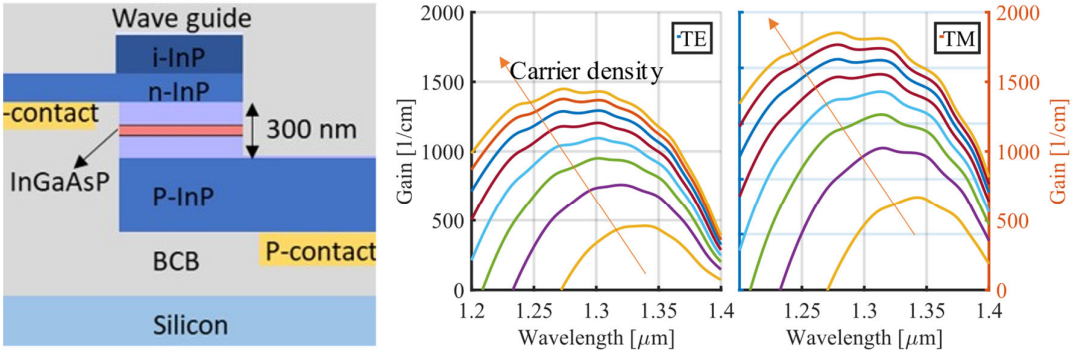

Figure 1 a) Cross-section of the SOA b) Material gain for TE (left axis) and TM (right axis)

3. SOA Gain and Gain Saturation

The gain provided by SOA depends on the SOA length, SOA width, and bias current. Primarily, the SOA wdth highly influences the gain saturation of the SOA. As we can see from equation 1, output saturation power is proportional to the effective mode area given by the ratio of waveguide width to confinement factor.

$$P_{o,sat} = \left(\frac{G_o \ln 2}{G_o - 2}\right) A \left(\frac{h\nu}{a\tau}\right) \quad (1)$$

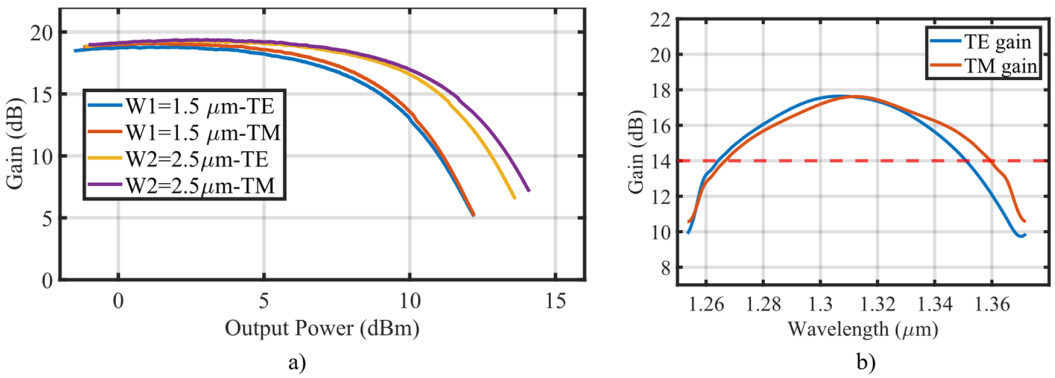

Figure 2 a) SOA gain for different SOA width b) TE and TM small-signal gain spectrum

Where G_0 is the unsaturated gain, hv is the photon energy, a is the differential gain, τ is the carrier lifetime, and $A=w/r$ is the amplifier effective modal area [6]. Fig. 2a depicts gain for SOA width of 1.5 µm and 2.5 µm at 5 kA/cm^2. A 500 µm long SOA gives an output saturation power of 11 dBm for 2.5 µm wide SOA, 2 dB more than the 1.5 µm. Fig. 2b shows a small-signal gain spectrum of 500 µm long and 2 µm wide SOA. We can see that it could provide over 60 nm 3 dB gain bandwidth at 4 kA/cm^2. The polarization sensitivity is < 0.5 dB.The TM gain curve reaches its peak at a higher wavelength because the tensile strain brings light holes closer to the conduction band, making TM transition happen at a higher wavelength

4. Switch architecture Modeling with the Designed SOA

Various optical switch architectures can be employed for optical switch realization, each having its pros and cons [10]. This study chooses Banyan and Hybrid Benes-Broadcast & select (HB-B&S) architectures to demonstrate optical switch functionality using the designed SOA. HB-B&S is a Benes architecture that uses a 4×4 B&S module instead of the 4×4 Benes, reducing 2 switching stages. Table 1 provides a summary of the different parameters of these architectures. The basic building block assumed for this analysis is a 2×2 B&S, and port count N is a power of 2.

Table 1 Parameters for Banyan and Hybrid Benes architectures

No.	Architecture	Number of MMI*	Number of SOAs*	Number of crossing*	Blocking?
1	Banyan	$2\log_2 N$	$\log_2 N$	$N-1$	Yes
2	HB-B&S	$4\log_2 N-4$	$2\log_2 N-3$	$2N-3$	No**

**in a path **rearrangeable non-blocking*

These architectures have also been emulated by representing path loss by variable optical attenuators (VOA) and reproducing SOA in the VPI photonics tool for system-level analysis. Fig. 3b shows path loss calculated from table 1 and the IMOS state-of-the-art loss values of 3.6 dB for MMI, 0.2 dB for crossing, 0.13 dB for bends and 1.8 dB/cm for waveguide [8], [9]. 16×16 Banyan and HB-B&S architectures having 3 and 4 SOA cascades, respectively, provide net on-chip gain assuming the SOA cascade can provide an average gain of 12 dB/SOA. Fig. 2a shows the case of Banyan architecture with typical values for the worst path. A transmission test with 4 WDM channels spaced at 400 GHz modulated with NRZ-OOK PRBS of bit length 2^{31} at 25 Gb/s on emulated 16×16 switches with different architectures has been performed. The result shows a power penalty of 1.5 dB and 2.25 dB for Banyan and HB-B&S, respectively, at a bit error ratio of 10^{-9}.

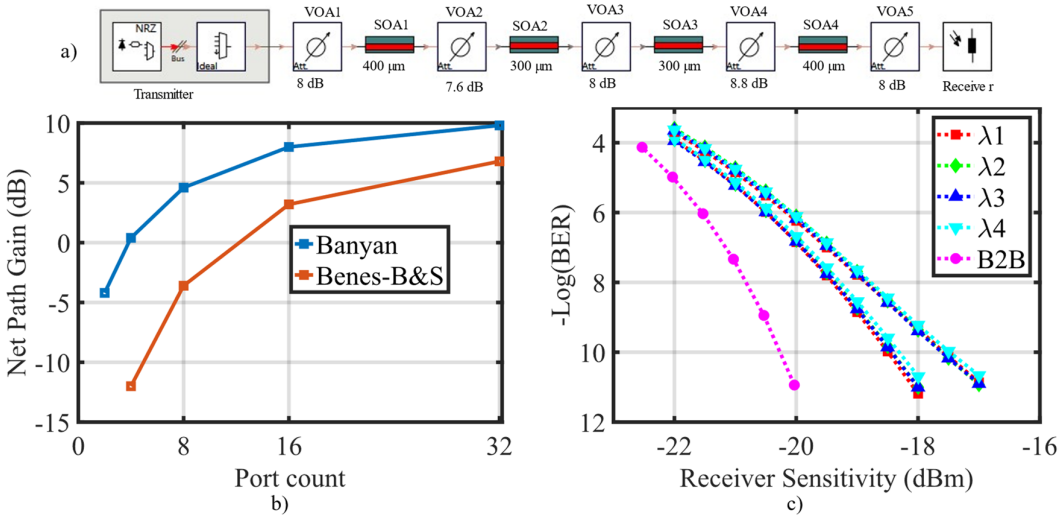

Figure 3 a) Banyan architecture setup with typical values for the worst (high loss) path b) Calculated path gain for Banyan and HB-B&S architectures c) Bite error rate for WDM transmission at 25 Gb/s.

3. Conclusion

We present the design of an O-band polarization-insensitive SOA in the IMOS platform. The obtained polarization insensitivity is sufficient to provide an acceptable polarization-insensitive operation. The obtained peak gain, output saturation power, polarization insensitivity of gain, and 3 dB gain bandwidth show the suitability of the designed SOA for polarization-insensitive SOA-based optical switch applications. The emulated switch architectures, Banyan and HB-B&S, show promising results for bit error rate, provide on-chip gain, and a reasonable number of on-chip components. In addition, the cascade of SOAs is long enough to mitigate the sensitivity power penalty. The choice between the two depends on whether a non-blocking architecture is needed.

4. Acknowledgement

This work is funded by European H2020 ICT TWILIGHT project (contract No. 781471) under the photonics PPP.

5. References

[1] Q. Cheng, S. Rumley, M. Bahadori, and K. Bergman, *Opt. Express*, vol. 26, no. 12, p. 16022, 2018.

[2] R. Stabile, A. Albores-Mejia, A. Rohit, and K. A. Williams, *Microsystems Nanoeng.*, vol. 2, no. November 2015, pp. 1–10, 2016, doi: 10.1038/micronano.2015.42.

[3] A. Rohit, J. Bolk, X. J. M. Leijtens, and K. A. Williams, *J. Light. Technol.*, vol. 30, no. 17, pp. 2913–2921, 2012, doi: 10.1109/JLT.2012.2208939.

[4] Q. Cheng, A. Wonfor, R. V. Penty, and I. H. White, *J. Light. Technol.*, vol. 31, no. 18, pp. 3077–3084, 2013, doi: 10.1109/JLT.2013.2278708.

[5] Y. Jiao *et al.*, *Semicond. Sci. Technol.*, vol. 36, no. 1, 2020, doi: 10.1088/1361-6641/abcadd.

[6] J. J. G. M. Van Der Tol *et al.*, *IEEE J. Sel. Top. Quantum Electron.*, vol. 24, no. 1, 2018, doi: 10.1109/JSTQE.2017.2772786.

[7] V. Pogoretskiy, J. van Engelen, J. van der Tol, A. Higuera-Rodriguez, M. Smit, and Y. Jiao, *Opt. InfoBase Conf. Pap.*, vol. Part F52-I, pp. 4–6, 2017, doi: 10.1364/IPRSN.2017.JW4A.1.

[8] Y. Jiao *et al.*, *Phys. Status Solidi Appl. Mater. Sci.*, vol. 217, no. 3, 2020, doi: 10.1002/pssa.201900606.

[9] J. Van Engelen, S. Reniers, J. Bolk, K. Williams, J. Van Der Tol, and Y. Jiao, *2019 Compd. Semicond. Week, CSW 2019 - Proc.*, no. 2019, 2019, doi: 10.1109/ICIPRM.2019.8819069.

[10] D. W. Feyisa, G. Patronas, P. Bakopoulos, N. Calabretta, and R. Stabile, pp. 2–3, 2021, doi: 10.1364/oe.26.016022.R.